Published in final edited form as:
J Neurosci. 2009 November 18; 29(46): 14408–14414. doi:10.1523/JNEUROSCI.0841-09.2009.

Schwann cells inhibit ectopic clustering of axonal sodium channels

Matthew G. Voas, **Thomas D. Glenn**, **Alya R. Raphael**, and **William S. Talbot***
Department of Developmental Biology, Stanford University School of Medicine, 279 Campus Dr., Stanford, CA 94305

Abstract

The clustering of voltage-gated sodium channels at the axon initial segment (AIS) and nodes of Ranvier is essential for the initiation and propagation of action potentials in myelinated axons. Sodium channels localize to the AIS through an axon-intrinsic mechanism driven by ankyrin G, while clustering at the nodes requires cues from myelinating glia that interact with axonal Neurofascin186 (Sherman et al., 2005; Dzhashiashvili et al., 2007; Yang et al., 2007). Here we report that in zebrafish mutants lacking Schwann cells in peripheral nerves (*erbb2*, *erbb3* and *sox10/colourless*), axons form numerous aberrant sodium channel clusters throughout their length. Morpholino knockdown of ankyrin G, but not Neurofascin, reduces the number of sodium channel clusters in Schwann cell-deficient mutants, suggesting that these aberrant clusters form by an axon-intrinsic mechanism. We also find that *gpr126* mutants, in which Schwann cells are arrested at the promyelinating stage (Monk et al., 2009), are deficient in the clustering of Neurofascin at the nodes of Ranvier. When Schwann cell migration in *gpr126* mutants is blocked, there is an increase in the number of Neurofascin clusters in peripheral axons. Our results suggest that Schwann cells inhibit the ability of ankyrin G to cluster sodium channels at ectopic locations, restricting its activity to the AIS and nodes of Ranvier.

Keywords

Schwann cell; sodium channel; ankyrin; node of Ranvier; axon initial segment; zebrafish

Introduction

The proper localization of voltage-gated sodium channels in axons is essential for normal neural function (Salzer et al. 2008). In myelinated axons, sodium channels are clustered in the short, unmyelinated gaps (nodes of Ranvier) that occur between the myelinated segments (internodes). This clustering of sodium channels at the nodes is essential for the rapid, saltatory conduction of action potentials that is characteristic of myelinated axons (Sherman et al., 2005). Sodium channels are also clustered at the base of the axon (the axon initial segment, or AIS), and this localization is required for the initiation of action potentials in many neurons (Khaliq and Raman, 2006; Palmer and Stuart, 2006).

Recent work describes two related, but distinct, mechanisms by which sodium channels form clusters in peripheral axons. In the first mechanism the myelinating glia (Schwann cells) present a ligand to discrete loci on the surface of underlying axons. This ligand stimulates the clustering of axonal Neurofascin, which in turn recruits sodium channels to the nascent cluster via ankyrin G. This “Neurofascin-dependent” mechanism is thought to be responsible for the clustering of

*Corresponding author: wtalbot@stanford.edu.

sodium channels at the nodes of Ranvier (Eshed et al., 2005; Sherman et al., 2005; Dzhashiashvili et al., 2007). In the second mechanism, ankyrin G forms clusters in the absence of glial input. Clustered ankyrin G then separately recruits sodium channels and Neurofascin. This "axon-intrinsic" mechanism is believed to initiate clustering of sodium channels at the AIS only (Dzhashiashvili et al., 2007; Yang et al., 2007).

While the importance of glia in establishing sodium channel clusters at nodes of Ranvier is well established, no study has examined axonal sodium channels in the complete absence of glia in vivo. In the zebrafish, mutants for *erbb2*, *erbb3* and *sox10* lack Schwann cells in peripheral nerves (Kelsh and Eisen 2000; Lyons et al. 2005; Pogoda et al. 2006). Here we report the unexpected finding that numerous abnormal sodium channel clusters form throughout the length of nerves that lack Schwann cells. Morpholino studies provide evidence that these abnormal clusters require ankyrin G, but not Neurofascin, implying that the axon-intrinsic mechanism of clustering that normally functions at the AIS can act ectopically in the absence of Schwann cells. We also find that Neurofascin clusters at the nodes of Ranvier are severely reduced in *gpr126* mutants, in which Schwann cells associate with axons but arrest at the promyelinating stage (Monk et al., 2009); this result suggests that Schwann cells stimulate clustering at nodes at the onset of myelination in zebrafish, as has been shown in mammals (Salzer et al. 2008). Surprisingly, removal of Schwann cells from peripheral nerves actually increased the number of clusters present in *gpr126* mutants, providing evidence that Schwann cells inhibit clustering of node molecules at inappropriate locations. Based on these data, we propose a new role for Schwann cells in restricting axon-intrinsic sodium channel clustering to the AIS. This inhibitory function complements the well-established role of myelinating glia in promoting cluster formation at the nodes of Ranvier.

Materials and methods

Zebrafish stocks

The *erbb2*^{st61}, *erbb3*^{st48} and *gpr126*^{st49} mutant lines were isolated in genetic screens for defects in myelinated axons (Lyons et al., 2005; Pogoda et al., 2006; Monk et al., 2009). The *cls*^{t3} and *Tg(FoxD3:GFP)17* lines have been described (Kelsh and Eisen 2000; Gilmour et al. 2002).

Antibodies and immunofluorescence

The following antibodies and dilutions were used: mouse anti-acetylated tubulin (Sigma, 1:1,000), mouse anti-panNa_VCh (Sigma, 1:500), rabbit anti-FIGQY (gift of M. Rasband, 1:1,000), rabbit anti-Tyrosine Hydroxylase (Chemicon, 1:500), purified rabbit anti-ankyrin G (see below, 1:2,000), purified guinea pig anti-extracellular Neurofascin (see below, 1:20).

To raise antibodies against ankyrin G, a region of *ank3b*, one of two duplicate genes encoding ankyrin G in zebrafish (corresponding to nucleotides 2,437-3,252 of a predicted *ank3b* cDNA, accession XM_695014) was amplified by RT-PCR from adult zebrafish brain RNA. In this region, which corresponds to part of the spectrin-binding domain, the predicted Ank3a and Ank3b proteins are more than 80% identical. The resulting cDNA was ligated in-frame downstream of the Maltose Binding Protein (MBP) encoding region of pMAL-c2X (New England Biolabs). Purified fusion protein was used to raise antibodies in rabbits (Covance Immunology Services). The resulting immune serum was incubated with purified MBP that had been conjugated to Affigel (Biorad) to separate anti-MBP from the immune serum. Anti-MBP-depleted immune serum was then incubated with MBP-ankyrin G fusion protein conjugated to Affigel. Bound anti-ankyrin G was washed by standard procedures, then eluted with 0.2 M glycine pH 2.0 in 150 mM NaCl, and immediately neutralized with 0.1 volumes of 2 M Tris, pH 8.5. BSA was added to 30 mg/ml and the antibodies were dialyzed against

TBS. The purified antibodies detected multiple bands on immunoblots of adult brain, likely corresponding to different ankyrin G isoforms (Fig. S1).

Antibodies versus extracellular Neurofascin were raised and purified as described for anti-ankyrin G above with the following exceptions. A region of *neurofascin* encoding part of the mucin-like domain (corresponding to nucleotides 3,340-3,666 of the *neurofascin* cDNA, accession FJ669144) was amplified by RT-PCR from adult zebrafish brain RNA and ligated in frame into pMAL-c2X. Purified MBP-mucin domain fusion protein was used to immunize guinea pigs, and anti-extracellular Neurofascin was purified from immune serum by incubating with MBP-mucin domain conjugated Affigel.

Immunofluorescence was performed as described (Voas et al., 2007) except that before incubation with anti-ankyrin G or anti-extracellular Neurofascin antibodies, the skin of embryos was peeled away from the body after fixation to facilitate antibody penetration. All fluorescent images were taken using a Zeiss LSM 5 Pascal confocal microscope.

Morpholino oligonucleotides

Gene Tools synthesized the following anti-sense MO sequences.

ank3a MO: CTCTCTCTTCCCACCCGTACCTTTT

neurofascin MO: AAGGTTTCATCCATTCTCACGTTGG

The *ank3a* MO is predicted to hybridize to the exon/intron boundary that follows the first exon of the neural-specific transcript of *ank3a* (Kordeli et al. 1995). The *neurofascin* MO is predicted to hybridize to the exon/intron boundary that follows the sixth exon of *neurofascin*. MO were diluted in water and injected into embryos from *erbb2*$^{st61/+}$ intercrosses at the one-cell stage. For ank3a injections, 2 ng of MO was injected per embryo. For *neurofascin* MO, 1.5 ng was injected per embryo for the sodium channel and Neurofascin assays (Fig. 4). For TEM analysis, 2.5 ng of neurofascin MO was injected (Fig. S6). Control embryos were injected with water alone. The total volume injected per embryo was 1 nL in all cases.

Transmission electron microscopy

Embryos were prepared for TEM at 3 days post fertilization (dpf) essentially as described (Lyons et al., 2008). Images were collected using a JEOL TEM1230.

Western

To make crude lysate, an adult brain was ground in the presence of protease inhibitors, sample buffer, and reducing agent. The lysate was then passed through a 27-gauge needle, boiled for 5 minutes and centrifuged. SDS-PAGE and Western blotting were performed by standard procedures. The purified rabbit anti-ankyrin G antibody was used at a dilution of 1:2,000.

AG1478 drug treatment

AG1478 (CalBiochem) was applied at 17 hours post fertilization (hpf) to embryos from *gpr126*$^{st49/+}$ heterozygote intercrosses at a final concentration of 4 μM in embryo medium with 1% DMSO. The medium plus AG1478 was changed daily until 4 dpf. Mock treatment was performed by applying embryo medium with 1% DMSO only.

Results

Abnormal clusters of axonal proteins form in the absence of Schwann cells

From two screens for mutants with defects in myelinated axons, mutant alleles of *erbb2* and *erbb3* were isolated (Lyons et al., 2005). In these mutants, proliferation and migration of Schwann cells along growing axons is disrupted, causing a lack of immature and myelinating Schwann cells in peripheral nerves (Lyons et al., 2005; Pogoda et al., 2006). Previous work in zebrafish has shown that sodium channel clustering in the PNS normally only occurs in myelinated axons, while unmyelinated axons have diffusely localized sodium channels (Voas et al., 2007). By immunofluorescence, we found that abundant clusters of sodium channels form in the posterior lateral line nerve (PLLn) of *erbb2* and *erbb3* mutants at 5 days post-fertilization (dpf, Fig. 1 A-C). Unlike sodium channel clusters in the wild type, clusters in mutants are asymmetric and elongated, and tend to occur in groups within the nerve rather than being evenly distributed (Fig. 1 A-C). Also, the total number of clusters in mutants is reduced compared to the wild type (Fig. 2 A). Most of these clusters do not appear to occur at the AIS because they are distributed throughout the length of the nerve in the mutants (Fig. 2 B). The neuronal cell bodies that give rise to the PLLn remain tightly grouped at the ganglia in mutants, as they do in the wild type (Fig. S2), indicating that the majority of clusters occur distant from the axon initial segments of the PLLn. At the AIS of *erbb2* mutants, sodium channel clustering is similar to that seen in wild type siblings (Fig. 1 I-J), indicating that the abnormal clustering phenotype is restricted to axonal regions that are distal to the AIS. These data demonstrate that in the absence of Schwann cells, peripheral axons form aberrant clusters of sodium channels at a distance from the AIS.

To determine if the clustering phenotype in these mutants reflects the absence of Schwann cells, or if the loss of a specific *erbb2/3* function causes this phenotype, we examined another mutant that lacks Schwann cells in peripheral nerves. The zebrafish *colourless* mutant (*cls*, the ortholog of mammalian *sox10*) is also strongly deficient in the production of Schwann cells (Kelsh and Eisen, 2000; Gilmour et al., 2002). As in *erbb2* and *erbb3* mutants, *cls* mutants also form abnormal clusters of sodium channels in the PLLn (Fig. 1 D). The clusters in *cls* mutants have the same defects in morphology and distribution as *erbb2* and *erbb3* mutants (Fig. 1 D). From these data, we conclude that aberrant sodium channel clusters form in axons of mutants that lack Schwann cells.

Sodium channels in axonal clusters are known to co-localize with several other axonal molecules. Two of these molecules in particular, ankyrin G and Neurofascin, are thought to play critical roles in the assembly of sodium channel clusters (Salzer et al., 2008). We found that sodium channel clusters in *erbb2*, *erbb3*, and *cls* mutants also co-localize with clusters of ankyrin G and Neurofascin (Fig. 1 E-H, and data not shown). Given the importance of ankyrin G and Neurofascin in sodium channel clustering in mammals, their presence in sodium channel clusters in these mutants suggests that ankyrin G and Neurofascin may contribute to cluster initiation in Schwann-cell deficient peripheral nerves.

The absence of Schwann cells in the PLLn of *cls*, *erbb2*, and *erbb3* mutants has been previously described using a number of criteria (Kelsh and Eisen, 2000; Gilmour et al., 2002; Lyons et al., 2005; Pogoda et al., 2006). To further examine the ultrastructure of the mutant nerves, we performed transmission electron microscopy (TEM) on the PLLn of cls^{t3}, $erbb2^{st61}$, and $erbb3^{st48}$ mutants and wild type siblings at 3 dpf. As expected, all three mutants show the complete absence of Schwann cells associated with the PLLn, including immature and myelinating Schwann cells (Fig. 3 A-D). Consistent with previous reports (Gilmour et al., 2002; Lyons et al. 2005; Pogoda et al. 2006), axons are present, but sometimes defasciculated, in the mutants (Fig. 3B-D). The mutant nerves are frequently located in the skin in *cls*, *erbb2*, and *erbb3* mutants (Fig. 3 F and data not shown), instead of immediately beneath the

skin as occurs in the wild type (Fig. 3 E). Although the axons appear to have normal ultrastructure, the number of axons is reduced in *cls*, *erbb2*, and *erbb3* mutants (Fig. 3 G).

The PLLn contains both afferent and efferent axons (Ghysen and Dambly-Chaudiere, 2004). To determine if the aberrant clusters found in the PLLn of Schwann cell deficient mutants occur preferentially in afferent or efferent axons, we labeled *erbb2*^{st61} mutants and wild type siblings with anti-Neurofascin, and anti-Tyrosine Hydroxylase, which labels efferent axons in the zebrafish PLLn (Faucherre et al., 2009). We found that in both mutants and wild type siblings, most Neurofascin clusters are not associated with Tyrosine Hydroxylase-positive axons (Fig. S3), suggesting that these clusters most frequently occur on afferent axons.

Clustering of sodium channels in Schwann-cell deficient peripheral nerves depends upon ankyrin G but not Neurofascin

Ankyrin G has essential functions in the clustering of sodium channels at both the AIS and the nodes of Ranvier. To investigate the role of ankyrin G in clustering sodium channels in zebrafish, we used a morpholino oligonucleotide (MO) to disrupt the function of the *ank3a* gene, one of two genes encoding ankyrin G in zebrafish. We injected one-cell stage embryos from intercrosses of *erbb2*$^{st61/+}$ heterozygotes with an MO that targets the neural-specific transcript of *ank3a* (Kordeli et al., 1995). We found that the number of sodium channel clusters per PLLn in MO-injected wild type animals was 49% of that seen in water-injected wild type controls shortly after cluster formation begins at 72 hpf (Fig. 4 A). We also found that *ank3a* MO-injected embryos have variably reduced levels of sodium channel clustering at the AIS (compare Fig. S4 A and B to Fig. S4 D), which is consistent with ankyrin G's role in recruiting sodium channels to the AIS. At 80 hours post fertilization (hpf), the morphology of *ank3a* MO-injected embryos did not differ from that of water-injected controls (Fig. S5 A, B). The total number of axons and the number of myelinated axons in the PLLn did not differ between MO-injected embryos and water-injected embryos (Fig. S6 A, B, D, E), indicating that there is no developmental delay in *ank3a* MO-injected embryos. Sodium channel clusters were not completely eliminated in *ank3a* MO-injected embryos, perhaps because of the activity of the duplicate gene *ank3b*, or because the effective concentration of MO is reduced by 72 hpf, when clusters are readily assayed. These results indicate that ankyrin G is necessary for the formation of sodium channel clusters, and thus its function is conserved between zebrafish and mammals.

We next asked if ankyrin G is required for the formation of clusters in peripheral nerves that lack Schwann cells. In MO-injected *erbb2* mutants, we found only 40% of the sodium channel clusters per PLLn that are found in water-injected mutants (Fig. 4 A). These data provide evidence that ankyrin G is also required for the formation of clusters in Schwann-cell deficient peripheral nerves, suggesting that clustering in these mutants occurs by one of the known mechanisms that requires ankyrin G.

To determine if clustering in Schwann-cell deficient nerves occurs through the Neurofascin-dependent mechanism, we injected *erbb2* mutants and wild type siblings with an MO that targets the *neurofascin* gene. The MO did not affect gross morphology compared to water-injected controls (Fig. S5 A+C), and the number and myelination of PLLn axons were unaffected in *neurofascin* MO-injected embryos (Fig. S6 A, C-E). As expected, the *neurofascin* MO showed no effect on the ability of sodium channels to cluster at the AIS (Fig. S4 C, D). At other positions in the axons, however, sodium channel clusters were reduced: at 72 hpf, the number of clusters per PLLn in MO-injected wild type embryos is 46% of that in water-injected, wild-type controls (Fig. 4 A). This result is consistent with the observation that Neurofascin is required for clustering at nodes of Ranvier in peripheral nerves (Sherman et al., 2005). Neurofascin was undetectable by immunofluorescence in the remaining sodium channel clusters of morpholino-injected embryos (Fig. 4 B-F), which may indicate that even low levels of Neurofascin are sufficient to initiate some clustering at nodes of Ranvier in wild type

embryos. In contrast to wild type, morpholino-injected *erbb2* mutant embryos showed no reduction in sodium channel clustering compared to water-injected *erbb2* mutants (Fig. 4 A). From our morpholino analysis, we conclude that clustering of sodium channels in Schwann-cell deficient peripheral nerves requires the function of ankyrin G, but not Neurofascin. Thus, the mode of clustering in these Schwann cell-deficient nerves resembles the axon-intrinsic mechanism that normally functions at the axon initial segment.

Schwann cells restrict axon-intrinsic sodium channel clustering

The foregoing results provide evidence that an axon-intrinsic mechanism drives clustering throughout the length of peripheral nerves in the absence of Schwann cells (Fig. 2 B, 4 A). These data suggest that Schwann cells may have a role in restricting axon-intrinsic clustering to the AIS. To test this hypothesis, we examined how clustering of axonal molecules is affected in zebrafish *gpr126* mutants, in which Schwann cells associate with and migrate along axons normally (Fig. 5 A-B), then arrest at the promyelinating stage (Pogoda et al., 2006;Monk et al., 2009). The average number of Neurofascin clusters in the PLLn of *gpr126* mutants is reduced by 11-fold compared to wild type siblings (mean=22 with S.D.=7, and mean=245 with S.D.=30, respectively; Fig. 5 C-D, G). Moreover, the average number of clusters in the *gpr126* mutant PLLn is 4-fold lower than that found in the Schwann-cell deficient *erbb2* mutant nerves (mean=22 with S.D.=7, and mean=88 with S.D.=9, respectively; Fig. 5 G). These data demonstrate that peripheral nerves that lack Schwann cells have more clusters than peripheral nerves with Schwann cells that are arrested at the promyelinating stage. The marked reduction of Neurofascin clusters in *gpr126* mutants supports the conclusion that Schwann cells arrested at the promyelinating stage can inhibit axon-intrinsic clustering but cannot initiate clustering of Neurofascin at nodes of Ranvier.

An important issue in the interpretation of the *gpr126* mutant phenotype is the possibility that peripheral nerves in these mutants may not be competent to form clusters of axonal molecules. To determine if *gpr126* mutant axons can form clusters when Schwann cells are eliminated, we used the ErbB kinase inhibitor AG1478 to block Schwann cell proliferation and migration in *gpr126* mutants. When applied before Schwann cell precursors migrate from the cranial ganglia, AG1478 blocks the migration of Schwann cells along peripheral nerves, producing an *erbb2/3*-like phenotype (Lyons et al., 2005). We applied 4μM AG1478 to *gpr126* mutants and wild type siblings from 17 hpf to 4 dpf, and then assayed the formation of axonal clusters in the PLLn. Similar to *erbb2* and *erbb3* mutants, AG1478-treated wild type fish also form clusters of Neurofascin in the PLLn (Fig. 5 E). The mean number of Neurofascin clusters in AG1478-treated *gpr126* mutants is also comparable to that seen in *erbb2* mutants (61 with S.D.=9, and 88 with S.D.=9, respectively; Fig. 5 F and G). Importantly, AG1478-treatment increases the average number of Neurofascin clusters in *gpr126* mutants by 2.8-fold (Fig. 5 G). These experiments demonstrate that the presence of Schwann cells arrested at the promyelinating stage inhibits the formation of Neurofascin clusters in *gpr126* mutants.

Discussion

Our analysis shows that numerous axonal clusters of sodium channels, Neurofascin and ankyrin G are present throughout the length of peripheral nerves that lack Schwann cells. This analysis was possible in zebrafish because the Schwann-cell deficient *erbb2*, *erbb3* and *cls/sox10* mutants survive for several days beyond the onset of sodium channel clustering. Mammalian mutants for *Erbb2*, *Erbb3* and *Sox10* are also strongly deficient in Schwann cells, but these mutants die before sodium channel clustering can be observed (Riethmacher et al., 1997; Morris et al., 1999; Britsch et al., 2001). Several viable mammalian mutants with myelination defects have been analyzed for effects on the clustering of axonal proteins. These mutants generally show a direct positive relationship between the presence of myelin and number of

sodium channel clusters (reviewed by (Poliak and Peles, 2003). However, most of these examples are of hypomyelinating or demyelinating models, which typically have extensive contact between Schwann cells and axons at the time when sodium channel clusters are formed. A notable exception is the severe dystrophic mouse, which has a mutation in *laminin alpha 2* (*Lama2*^{dy}). In *Lama2*^{dy} mutants, large sections of peripheral nerves up to 10 or more millimeters in length lack Schwann cells (Bradley and Jenkison, 1973). By immunofluorescence and immuno-electron microscopy, Deerinck et al. found clusters of sodium channels in regions of peripheral nerves from *Lama2*^{dy} mutant mice that were devoid of Schwann cells (Deerinck et al., 1997). In these Schwann-cell deficient regions of peripheral nerves, sodium channels co-cluster with ankyrin G, and the clusters have elongated and asymmetric morphologies much like those we observe in zebrafish Schwann-cell deficient mutants (Fig. 1; (Deerinck et al., 1997). The formation of clusters in Schwann-cell deficient regions of *Lama2*^{dy} peripheral nerves suggests that Schwann cells have a conserved function in the inhibition of ectopic axon-intrinsic clustering in zebrafish and mammals. This function may allow myelinating Schwann cells to inhibit inappropriate sodium channel clusters at the internode.

The observation that sodium channel clusters, albeit abnormal ones, are present in mutants deficient in Schwann cells (Deerinck et al., 1997; this work) appears to contrast with studies that detected no sodium channel clusters in axons of cultured mammalian dorsal root ganglion (DRG) neurons. For example, Eshed et al. found that DRG axons in the absence of Schwann cells do not form clusters of Neurofascin or sodium channels unless the Neurofascin-binding domain of the Schwann cell ligand Gliomedin is added to the culture (Eshed et al., 2005). This discrepancy may indicate that there are important differences between experiments performed in culture and those performed in vivo. Nonetheless, culture studies and in vivo analyses in mouse and zebrafish all support an essential role for cues from myelinating Schwann cells in establishing the sodium channel clusters that are characteristic of the mature node of Ranvier (Salzer et al. 2008; this work).

Previous work has shown that Schwann cells normally promote sodium channel clustering at nodes, and here we demonstrate that Schwann cells inhibit axon-intrinsic clustering outside of nodes and the AIS (summarized in Fig. S7). It is possible that these seemingly contradictory functions reflect a dual role for Schwann cell derived cues in the regulation of ankyrin G. While ankyrin G is known to initiate sodium channel clustering at the AIS, it also plays an essential role in the Neurofascin-dependent pathway that functions at the nodes of Ranvier (Dzhashiashvili et al., 2007). The biochemical function of ankyrin G is similar at the AIS and at nodes, so perhaps the primary effect of clustering Neurofascin at nodes of Ranvier is to activate the axon-intrinsic mechanism of sodium channel clustering at discrete loci. This convergence of extrinsic and intrinsic factors may ensure the rapid reorganization of axonal proteins so that there is no loss of axonal function during the transition from continuous to saltatory modes of conduction.

In conclusion, we have shown that in the absence of Schwann cells, axonal proteins form clusters in an ankyrin G-dependent manner. Additionally, Schwann cells must transition from the promyelinating stage to the myelinating stage before they stimulate the normal clustering of sodium channels that is characteristic of the node of Ranvier. The presence of axonal clusters in the absence of Schwann cells reveals a role for Schwann cells in the inhibition of axon-intrinsic mechanisms of clustering.

Supplementary Material

Refer to Web version on PubMed Central for supplementary material.

Acknowledgments

We thank Matthew Rasband for providing the FIGQY antibody and members of our laboratory for helpful discussion and comments on the manuscript. M. G. V. was supported by a fellowship from the NIH. T. D. G. and A. R. R. were supported by an NIH training grant. This work was supported by grants to W. S. T. from the NMSS (RG3943-A-2) and the NIH (NS050223).

References

Bradley WG, Jenkison M. Abnormalities of peripheral nerves in murine muscular dystrophy. J Neurol Sci 1973;18:227–247. [PubMed: 4120487]

Britsch S, Goerich DE, Riethmacher D, Peirano RI, Rossner M, Nave KA, Birchmeier C, Wegner M. The transcription factor Sox10 is a key regulator of peripheral glial development. Genes Dev 2001;15:66–78. [PubMed: 11156606]

Deerinck TJ, Levinson SR, Bennett GV, Ellisman MH. Clustering of voltage-sensitive sodium channels on axons is independent of direct Schwann cell contact in the dystrophic mouse. J Neurosci 1997;17:5080–5088. [PubMed: 9185545]

Dzhashiashvili Y, Zhang Y, Galinska J, Lam I, Grumet M, Salzer JL. Nodes of Ranvier and axon initial segments are ankyrin G-dependent domains that assemble by distinct mechanisms. J Cell Biol 2007;177:857–870. [PubMed: 17548513]

Eshed Y, Feinberg K, Poliak S, Sabanay H, Sarig-Nadir O, Spiegel I, Bermingham JR Jr, Peles E. Gliomedin mediates Schwann cell-axon interaction and the molecular assembly of the nodes of Ranvier. Neuron 2005;47:215–229. [PubMed: 16039564]

Faucherre A, Pujol-Marti J, Kawakami K, Lopez-Schier H. Afferent neurons of the zebrafish lateral line are strict selectors of hair-cell orientation. PLoS One 2009;4:e4477. [PubMed: 19223970]

Ghysen A, Dambly-Chaudiere C. Development of the zebrafish lateral line. Curr Opin Neurobiol 2004;14:67–73. [PubMed: 15018940]

Gilmour DT, Maischein HM, Nusslein-Volhard C. Migration and function of a glial subtype in the vertebrate peripheral nervous system. Neuron 2002;34:577–588. [PubMed: 12062041]

Jessen KR, Mirsky R. The origin and development of glial cells in peripheral nerves. Nat Rev Neurosci 2005;6:671–682. [PubMed: 16136171]

Kelsh RN, Eisen JS. The zebrafish colourless gene regulates development of non-ectomesenchymal neural crest derivatives. Development 2000;127:515–525. [PubMed: 10631172]

Khaliq ZM, Raman IM. Relative contributions of axonal and somatic Na channels to action potential initiation in cerebellar Purkinje neurons. J Neurosci 2006;26:1935–1944. [PubMed: 16481425]

Kordeli E, Lambert S, Bennett V. AnkyrinG. A new ankyrin gene with neural-specific isoforms localized at the axonal initial segment and node of Ranvier. J Biol Chem 1995;270:2352–2359. [PubMed: 7836469]

Lyons DA, Naylor SG, Mercurio S, Dominguez C, Talbot WS. KBP is essential for axonal structure, outgrowth and maintenance in zebrafish, providing insight into the cellular basis of Goldberg-Shprintzen syndrome. Development 2008;135:599–608. [PubMed: 18192286]

Lyons DA, Pogoda HM, Voas MG, Woods IG, Diamond B, Nix R, Arana N, Jacobs J, Talbot WS. *erbb3* and *erbb2* are essential for Schwann cell migration and myelination in zebrafish. Curr Biol 2005;15:513–524. [PubMed: 15797019]

Monk KR, Naylor SG, Glenn TD, Mercurio S, Perlin JR, Dominguez C, Moens CB, Talbot WS. A G protein-coupled receptor is essential for Schwann cells to initiate myelination. Science 2009;325:1402–1405. [PubMed: 19745155]

Morris JK, Lin W, Hauser C, Marchuk Y, Getman D, Lee KF. Rescue of the cardiac defect in ErbB2 mutant mice reveals essential roles of ErbB2 in peripheral nervous system development. Neuron 1999;23:273–283. [PubMed: 10399934]

Palmer LM, Stuart GJ. Site of action potential initiation in layer 5 pyramidal neurons. J Neurosci 2006;26:1854–1863. [PubMed: 16467534]

Pogoda HM, Sternheim N, Lyons DA, Diamond B, Hawkins TA, Woods IG, Bhatt DH, Franzini-Armstrong C, Dominguez C, Arana N, Jacobs J, Nix R, Fetcho JR, Talbot WS. A genetic screen

identifies genes essential for development of myelinated axons in zebrafish. Dev Biol 2006;298:118–131. [PubMed: 16875686]

Poliak S, Peles E. The local differentiation of myelinated axons at nodes of Ranvier. Nat Rev Neurosci 2003;4:968–980. [PubMed: 14682359]

Riethmacher D, Sonnenberg-Riethmacher E, Brinkmann V, Yamaai T, Lewin GR, Birchmeier C. Severe neuropathies in mice with targeted mutations in the ErbB3 receptor. Nature 1997;389:725–730. [PubMed: 9338783]

Salzer JL, Brophy PJ, Peles E. Molecular domains of myelinated axons in the peripheral nervous system. Glia 2008;56:1532–1540. [PubMed: 18803321]

Sherman DL, Tait S, Melrose S, Johnson R, Zonta B, Court FA, Macklin WB, Meek S, Smith AJ, Cottrell DF, Brophy PJ. Neurofascins are required to establish axonal domains for saltatory conduction. Neuron 2005;48:737–742. [PubMed: 16337912]

Voas MG, Lyons DA, Naylor SG, Arana N, Rasband MN, Talbot WS. alphaII-spectrin is essential for assembly of the nodes of Ranvier in myelinated axons. Curr Biol 2007;17:562–568. [PubMed: 17331725]

Yang Y, Ogawa Y, Hedstrom KL, Rasband MN. betaIV spectrin is recruited to axon initial segments and nodes of Ranvier by ankyrinG. J Cell Biol 2007;176:509–519. [PubMed: 17283186]

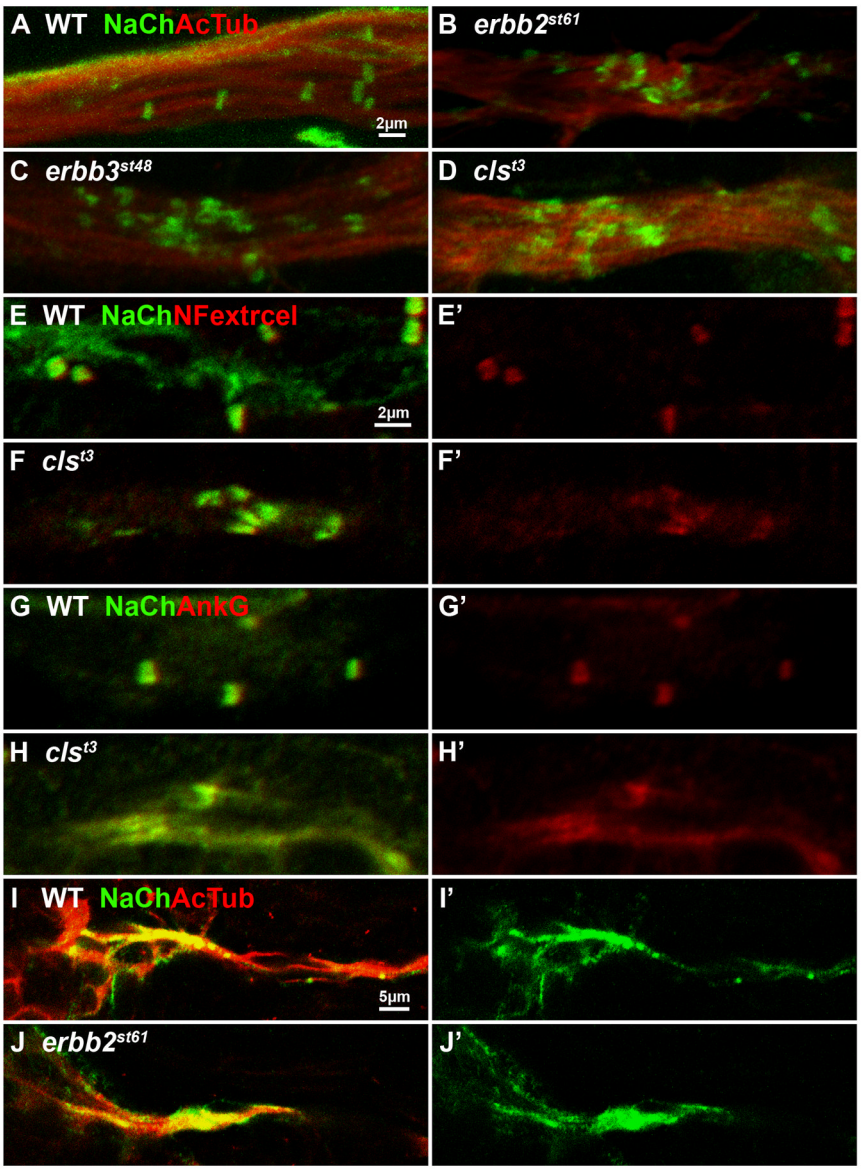

Figure 1. In the absence of Schwann cells, peripheral axons form aberrant clusters of sodium channels, NF186 and ankyrin G

(A-D) Whole-mount immunofluorescent labeling of sodium channels (anti-panNa_vCh, green) and axons (anti-acetylated tubulin, red) in wild type (A), *erbb2*^{st61} (B), *erbb3*^{st48} (C), and *cls*^{t3} (D) mutants at 5 dpf reveals the presence of clusters in the PLLn of Schwann-cell deficient mutants. **(E-F)** Immunofluorescent labeling of sodium channels (green) and the extracellular domain of Neurofascin (red) in the PLLn of *cls*^{t3} mutants and wild type siblings. **(G-H)** Sodium channels (green) and ankyrin G (red) in the PLLn of *cls*^{t3} mutants and wild type siblings. **(I-J)** Immunofluorescently labeled sodium channels (green) and acetylated tubulin (red) at the AIS of multiple PLLn axons in wild type (I) and *erbb2*^{st61} (J) embryos at 3 dpf.

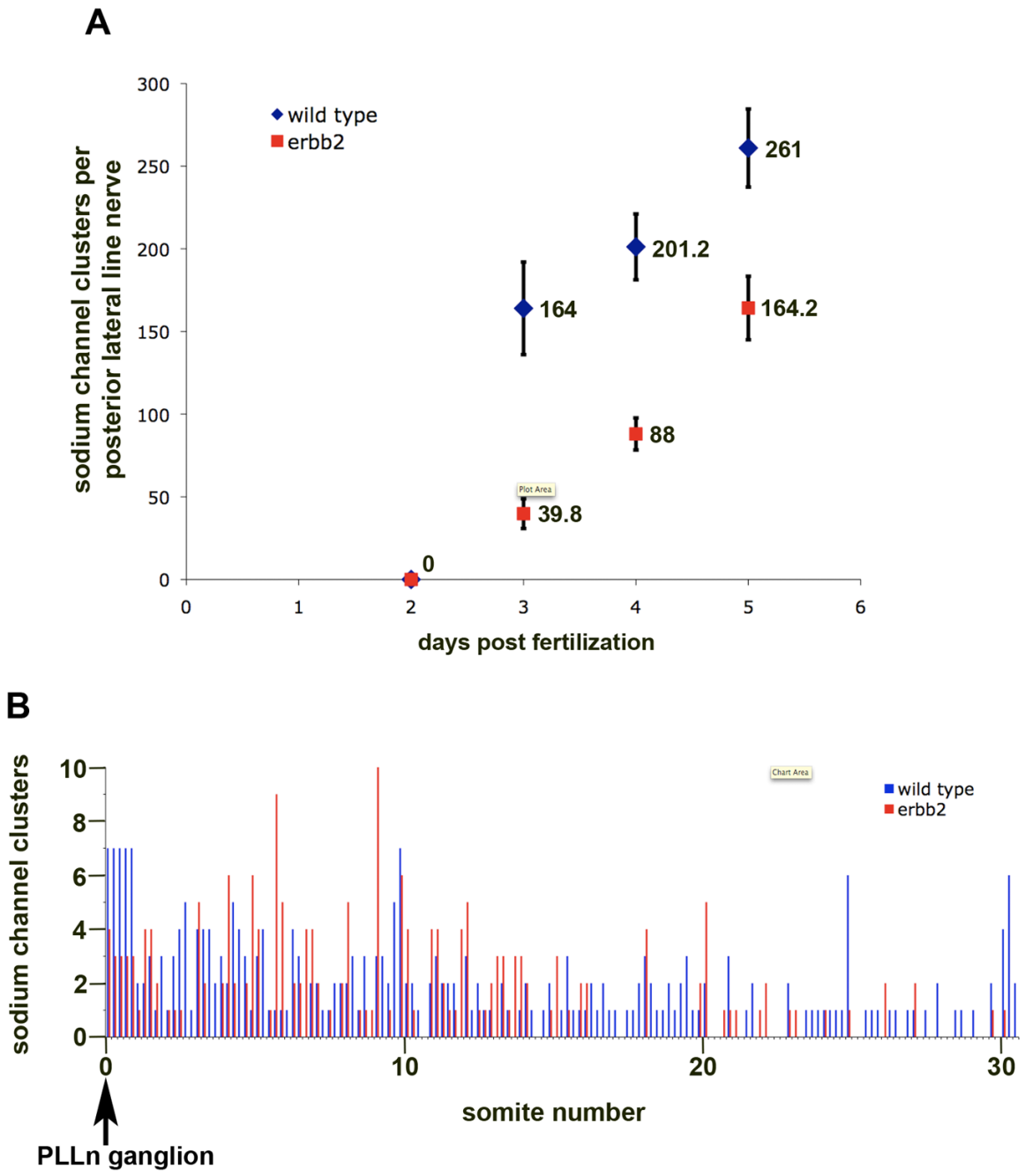

Figure 2. In the absence of Schwann cells, peripheral axons form numerous sodium channel clusters throughout their length

(A) The total number of sodium channel clusters per PLLn is shown from 2 dpf to 5 dpf for *erbb2*^{st61} mutants (red) and wild type siblings (blue). Error bars indicate +/- one S.D. For each data point, 5 PLLn were scored from different fish. **(B)** The positions of sodium channel clusters in the PLLn of one *erbb2*^{st61} mutant (red) and one wild type sibling (blue) at 5 dpf were recorded using the underlying somitic boundaries as landmarks. The position of the PLLn ganglion, which is found near the origin of the first somite, is indicated. Each data point represents the number of PLLn clusters that overlie each one-fifth of a somite. Similar results have been observed in *erbb3*^{st48} and in *cls*^{t3} mutants (data not shown).

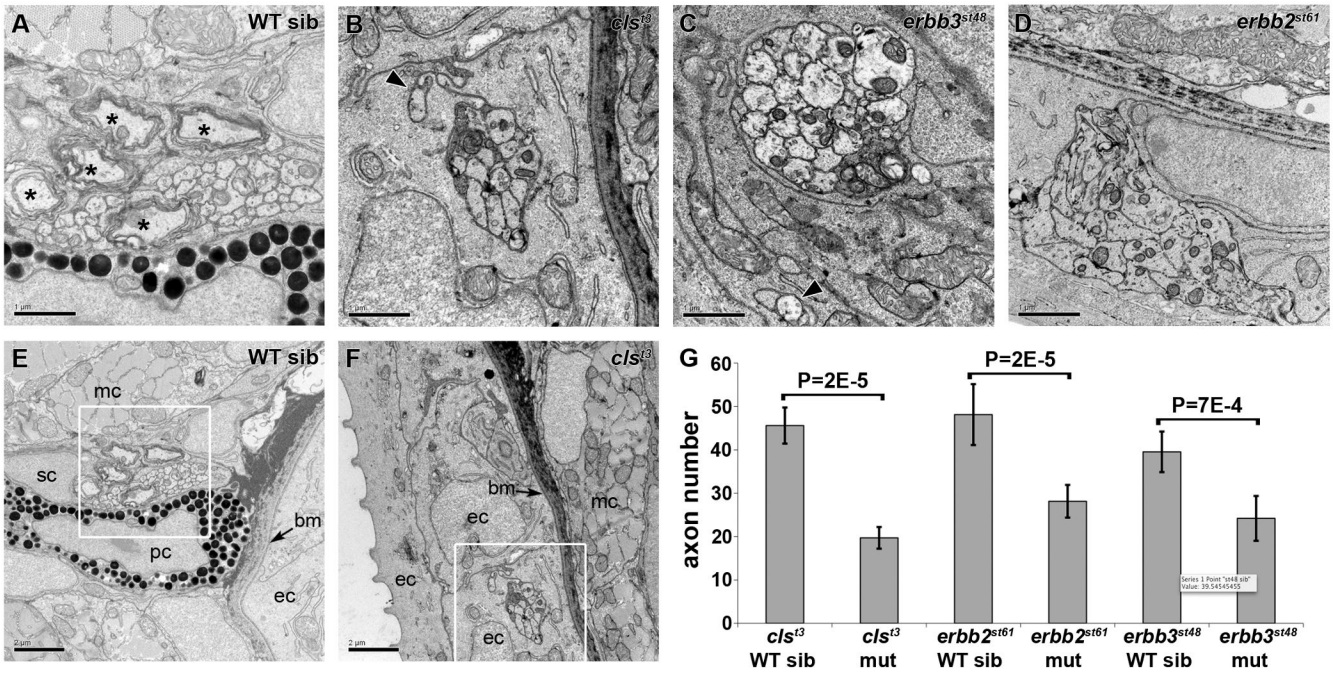

Figure 3. *cls*^{t3}, *erbb2*^{st61}, and *erbb3*^{st48} mutants lack Schwann cells and have fewer PLLn axons

(A) TEM of the PLLn from a wild type sibling at 3 dpf reveals the presence of several myelinated axons (asterisks). **(B-D)** *cls*^{t3} mutant (B), *erbb3*^{st48} mutant (C), and *erbb2*^{st61} mutant (D) embryos at 3 dpf completely lack myelin and recognizable Schwann cells. It is common for axons from these mutant nerves to become defasciculated (arrowheads in B and C). **(E)** In the wild type, the PLLn is normally located beneath the skin, adjacent to muscle cells. The basement membrane (arrow) separates the PLLn from the epidermal cells of the skin. **(F)** In Schwann-cell deficient embryos, the PLLn is frequently located superficial to the basement membrane. Scale bars represent 1 μm in A-D and 2 μm in E and F. Boxed areas in E and F indicate the region shown in A and B, respectively. **(G)** Quantification of axon number in wild type siblings and *cls*^{t3}, *erbb2*^{st61}, and *erbb3*^{st48} mutants. The P values for unpaired t-test comparisons (two-tailed) are shown. The following number of nerves were scored: *cls*^{t3} sib – 5 nerves from 3 embryos; *cls*^{t3} mut – 7 nerves from 4 embryos; *erbb2*^{st61} sib – 8 nerves from 5 embryos; *erbb2*^{st61} mut – 7 nerves from 4 embryos; *erbb3*^{st48} sib – 11 nerves from 6 embryos; and *erbb3*^{st48} mut – 5 nerves from 3 embryos. Error bars represent +/- one standard deviation. Abbreviations: mc, muscle cell; sc, Schwann cell; pc, pigment cell; ec, epidermal cell; bm, basement membrane.

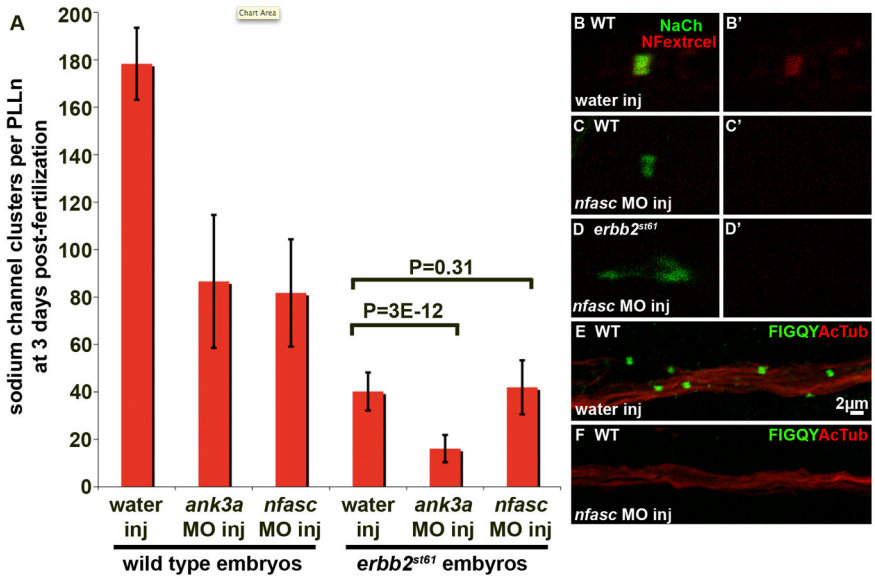

Figure 4. Sodium channel clustering in Schwann-cell deficient peripheral nerves is inhibited by knockdown of ankyrin G but not Neurofascin

(A) Embryos from *erbb2*$^{st61/+}$ heterozygous intercrosses were injected with water, or with MO against the neural-specific transcript of *ank3a*, or with MO against *neurofascin*. The average number of sodium channel clusters per PLLn is shown at 72 hpf (error bars indicate +/- one S.D.). The P values for unpaired t-test (single-tailed) comparisons are shown. One PLLn was scored per embryo and the number of embryos scored from left to right is 18, 20, 20, 15, 20, and 21. **(B-D)** Water-injected wild type sibling (B), *nfasc* MO-injected wild type sibling (C), and *nfasc* MO-injected *erbb2*^{st61} mutant (D) at 72 hpf, immunolabeled with anti-panNa_VCh (green) and anti-extracellular Neurofascin (red). Neurofascin is shown alone in B′-D′. **(E-F)** Wild type 72 hpf embryos injected with water (E) or *neurofascin* MO (F) labeled with anti-acetylated tubulin (red) and anti-FIGQY (recognizes intracellular epitope of Neurofascin, green).

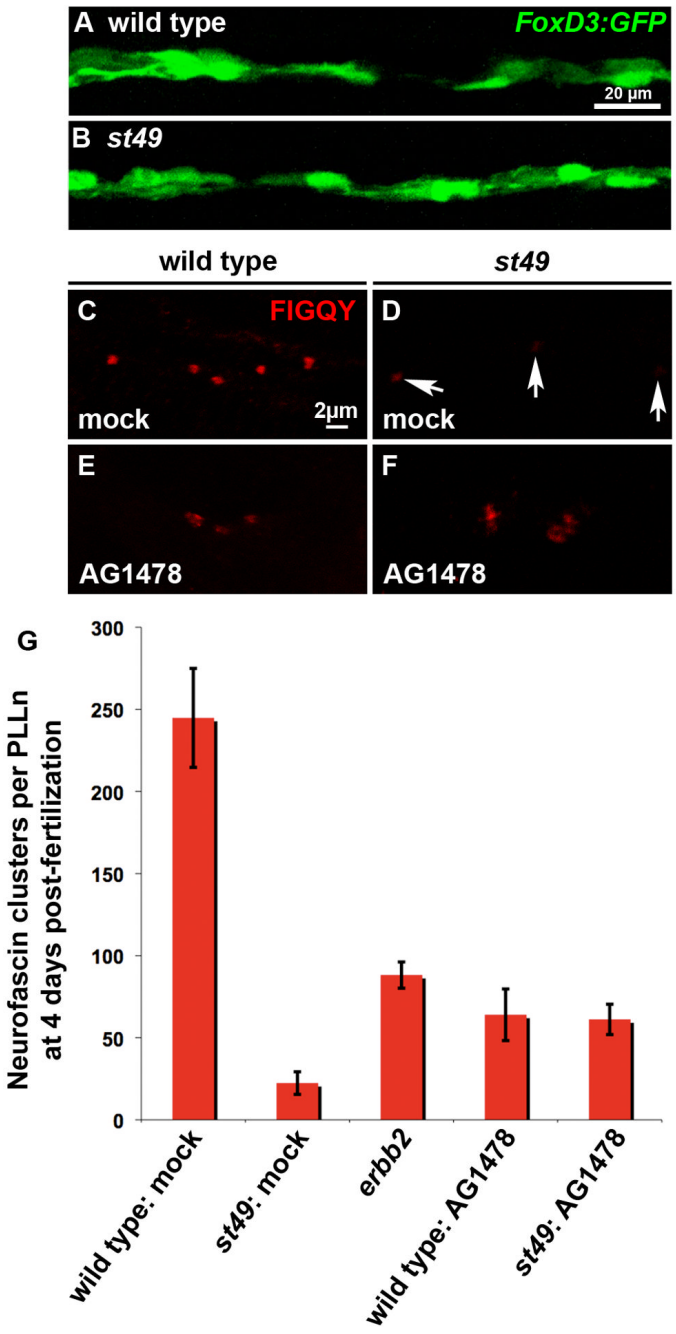

Figure 5. Schwann cells arrested at the promyelinating stage inhibit Neurofascin clusters

(A-B) Schwann cells labeled by a *FoxD3:GFP* transgene are present in wild type siblings (A) and *gpr126*^{st49} mutants at 5 dpf. (B). **(C-G)** Neurofascin clusters were scored in the PLLn of mock-treated wild type siblings (C, G), mock-treated *gpr126*^{st49} mutants (D, G), AG1478-treated wild type siblings (E, G), and AG1478-treated *gpr126*^{st49} mutants (C, G) using anti-FIGQY at 4 dpf. Arrows in D mark weakly labeled clusters in the *gpr126* mutant. In G, one PLLn was scored per embryo, and the number of embryos scored from left to right is 5, 5, 5, 12 and 11.